Exact computation of the spectra of periodic Schrödinger operators, and electronic states of modulated superlattices

Giorgio Mantica
Service de Physique Théorique, CE-Saclay, F-91191, Gif-sur-Yvette CEDEX, France

Stefano Mantica
Dipartimento di Fisica Generale A. Volta, Università di Pavia, Pavia, Italy
(Received 17 December 1990; revised manuscript received 13 September 1991)

A general method for computing the spectra of periodic Schrödinger operators is introduced here. The method is based on the classical theory of moments, and provides exact, rapidly converging bounds to the energy bands of periodic Hamiltonian operators, in any number of space dimensions. As an illustration of the general theory, we develop an application to the electronic states of modulated superlattices, in the envelope-function approximation. This allows one to obtain important information on the effects of variable effective mass and relative-band-offset ratio in these materials.

I. INTRODUCTION

When the potential $V(r)$ is periodic: $V(\mathbf{r}+\mathbf{T}) = V(\mathbf{r})$, for a group of translations $\mathcal{T}$, $\mathbf{T} \in \mathcal{T}$, the Hamiltonian

$$H = -\frac{\hbar^2}{2}\left(\nabla\frac{1}{m}\nabla\right) + V(\mathbf{r}), \tag{1}$$

is a periodic Schrödinger operator. The operator ∇ represents the derivative with respect to the components of $\mathbf{r} \in \mathbb{R}^d$, and (1) has been ordered in such a way that H is an apparently symmetric operator, even for a mass m depending on $\mathbf{r}$.[1,2] We will generally assume also that $m(\mathbf{r})$ is invariant under the action of the translation group $\mathcal{T}$. This exactly corresponds to the case of modulated superlattices, as will be seen later.

Thanks to the Bloch-Floquet theorem, the spectral properties of H can be obtained by "fiber integral" decomposition:[3] that is, by posing $\psi = \exp\{i\mathbf{k}\cdot\mathbf{r}\}\, u_{\mathbf{k}}(\mathbf{r})$, the eigenvalue equation $H\psi = E_{\mathbf{k}}\psi$ becomes

$$-\frac{\hbar^2}{2m}(-k^2 + 2i\mathbf{k}\cdot\nabla + \nabla^2)\, u_{\mathbf{k}} + \frac{\hbar^2}{2m^2}(\nabla m)\cdot(i\mathbf{k}+\nabla)\, u_{\mathbf{k}} + (V - E_{\mathbf{k}})\, u_{\mathbf{k}} = 0, \tag{2}$$

where $u_{\mathbf{k}}(\mathbf{r})$ has the periodicity given by the translation group $\mathcal{T}$. The second term on the left-hand side is null in the ordinary case of constant mass. The eigenvalues $E_{\mathbf{k}}$ draw the energy bands, as $\mathbf{k}$ ranges in the first Brillouin zone in reciprocal space: the aim of this paper is to show that the eigenfunctions $u_{\mathbf{k}}$ and the related eigenenergies $E_{\mathbf{k}}$ can be rigorously computed via a moment method technique.

This technique starts out from a Fourier space representation of $u_{\mathbf{k}}$ and employs a linearized version of the Toeplitz inequalities for the Fourier components (also called trigonometric moments) of any positive function. Contrary to most Fourier methods, this allows us to compute *exact, rapidly converging upper and lower bounds* to the energy bands: $E_<(\mathbf{k}) < E_{\mathbf{k}} < E_>(\mathbf{k})$ for any value of the wave vector $\mathbf{k}$. We now illustrate the key steps in this approach, which follows from general moment method techniques (see Ref. 4 and references therein).

The one-dimensional case with $k = 0$, and m constant (which has been partly anticipated in Ref. 4) is particularly simple, and can be used for illustrative purposes. Here, Eq. (2) simplifies to

$$-\frac{\hbar^2}{2m}\nabla^2\, u + (V - E)\, u = 0, \tag{3}$$

with $u(r) = u(r+T)$. Its solutions u can be taken to be real functions. The basic ingredients of our construction are the *trigonometric moments* u_n of such solutions, defined by

$$u_n = \frac{1}{T}\int_0^T e^{ingr} u(r)\, dr, \tag{4}$$

where T is the period of the potential, and $g = 2\pi/T$. It is immediate that such moments are the coefficients of the Fourier expansion of $u(r)$. Due to periodicity, the potential $V(r)$ can also be expressed as a Fourier summation:

$$V(r) = \sum_l v_l\, e^{-ilgr}. \tag{5}$$

By inserting the trigonometric expansions for V and u into Eq. (3) one transforms the eigenvalue problem, for any given k, into an infinite set of algebraic equations for the moments u_n. This formulation is exactly equivalent to the original problem, and as hard to solve; nevertheless, in the common case where a *finite* number of harmonics appears in the potential expansion (5), a recursive solution is possible: u_n can be obtained as a (recur-

sive) function of the energy E, the Fourier components of the potential $\mathbf{v}$, and a finite set of *missing* moments u_j, $j = 0, \ldots, I$, which are needed to initialize the recursion relation:

$$u_n = F_n(u_0, \ldots, u_I; E; \mathbf{v}). \tag{6}$$

For instance, if $V = 2v_1 \cos(gr)$, Eq. (3) becomes a Mathieu equation, for which one obtains

$$\frac{\hbar^2}{2m} n^2 g^2 u_n + v_1 u_{n+1} + v_1 u_{n-1} - E u_n = 0$$

$$\text{with } -\infty \leq n \leq \infty. \tag{7}$$

Assuming u to be even (the odd case is equivalently treated) one has $u_n = u_n^* = u_{-n}$ and hence

$$u_1 = \frac{1}{2v_1} E u_0,$$

$$u_2 = \frac{1}{2v_1^2} \left(E - \frac{\hbar^2 g^2}{2m} \right) E u_0 - u_0, \tag{8}$$

etc. All moments are then functions of E and u_0. This is a particular case of Eq. (6) with $I = 0$. In Eq. (6), the eigenenergy E and the missing moments are still undetermined. [The particular case (8) is easier, as a single missing moment can always be determined via a normalization condition.]

The final and crucial step in the theory comes after noticing that, $u(r)$ being real continuous and periodic, there exists a suitable constant Q in such a way that $f(r) = u(r) + Q$ is positive. As a consequence, the moments $f_n = u_n + Q\delta_{n,0}$ are bound to satisfy a stringent set of inequalities, obtained via the Toeplitz matrices of rank M with entries $T_{ij} = f_{i-j}$, $i, j = 0, \ldots, M-1$. The required inequalities are $\det(T) \geq 0$, for any M.[4,15]

We will show that a suitable linearization of such inequalities, which involve the missing moments and the eigenenergy via Eq. (6), provides exact bounds for the allowed values of such unknown quantities, and reconstruct both the spectrum E, and the eigenfunction $u(r)$. For instance, taking $Q = 0$ in the previous example the ground state is uniquely identified as the only eigenstate whose eigenfunction has no nodes. Then, the inequality for $M = 2$ reads

$$T_{00}T_{11} - T_{01}T_{10} = u_0^2 - u_1^2 \geq 0,$$

and inserting the value of u_1 one obtains bounds for the ground-state energy E_0: $|E_0| \leq 2|v_1|$. Increasing M leads to exponentially convergent bounds, as observed in Ref. 4.

This procedure recommends itself for many reasons: first of all, it produces rigorous bounds to the spectral properties, and, as such, can be used to test other solution procedures. Moreover, it provides a fully constructive solution of the spectral problem for the wide class of systems mentioned above. We will exemplify this technique via its application to an interesting physical problem: the determination of the electronic states of superlattices in the so-called *envelope-function* approximation.[5,6] To end this Introduction, let us show how these can be described via a Hamiltonian of the form (1).

A superlattice is a material composed of two or more different crystalline solids, which are arranged in a periodic fashion. Two fundamental length scales characterize such a system: the atomic period of the elementary constituents (typically a few angstroms), and the "superperiod," that is, the periodicity of the man-made composed material, which can be of the order of hundreds of angstroms. A typical example is given by a structure where N_A atomic layers of solid A, are followed by N_B layers of solid B, and so on by periodicity.

Because the superperiod is one or two orders of magnitude larger than the intrinsic periods of the crystalline solids, a set of tight "minibands" is created, which are highly desirable for the design of ultrafast electronic components.[7] As a first approximation, one can think of the (conduction and valence) bands of the different materials as producing a sequence of square-well potentials,[8] which have been appropriately called "man-made quantum wells." Minibands are then given by the quantum states of particles (electron and holes) confined in such wells.

A more general shape of superlattice can be considered, as illustrated in the following example: via the molecular-beam epitaxy (MBE) technique,[9] it is possible to build a structure composed of successive layers of the crystalline semiconductor $Al_xGa_{1-x}As$, where the alloy ratio of aluminum, x, can be varied from layer to layer. In this way, a "modulated" specimen is produced, where, for instance, x is a sinusoidal function of the growth coordinate of the superlattice. Since the energy gaps can be assumed to vary also proportionally with x (see the discussion in Sec. IV), this system can be rendered by the Hamiltonian (1), where $m(\mathbf{r})$ is the local effective mass, $V(\mathbf{r})$ is proportional to the local direct energy gap of $Al_xGa_{1-x}As$, and $\mathbf{k}$ ranges in the first Brillouin zone of the superstructure.

When applied to this problem, our technique allows us to study the influence of significant physical parameters, namely, the band-offset energy[10] and the position-dependent effective mass. To our knowledge this latter has been treated up to now only by perturbative methods or via square-well approximations.[5,11]

It is important to remark at this point that our method is not conceived to be applied to square wells, Kronig-Penney (KP) -type potentials, which allow for an efficient transfer-matrix-based computation of its spectral quantities: this technique is straightforward, precise,[12] and does not require the mathematical sophistication presented in this paper. In fact, the trigonometric moment technique developed here is not the most well-suited to deal with such traditional superlattices (truncation of the infinite Fourier series corresponding to periodic square wells is possible, but not optimal). If rigorous upper and lower bounds for KP potentials are needed, a different moment method technique (*not* based on trigonometric moments) can nevertheless be developed, following, e.g., the lines of Ref. 13.

The scheme of this paper is the following: in Sec. II

the general formalism for periodic Schrödinger operators is explained in detail. The Toeplitz inequalities are introduced, as well as their (infinitely many) linearizations. It is shown how to employ these inequalities to obtain bounds to the spectral properties. In Sec. III we treat the illustrative example of modulated semiconductor superlattices, obtaining explicit formulas to enter the general framework of Sec. II. In Sec. IV we show the numerical results obtained for two realistic examples of superlattices, and we comment on their physical significance. Finally, we compare our exact predictions with numerical results obtained by a more traditional Fourier technique.

II. GENERAL FORMALISM FOR PERIODIC OPERATORS

We develop in this section the general formalism for periodic Schrödinger operators, in a generic d-dimensional space. The general solution $u_{\mathbf{k}}(\mathbf{r})$ of Eq. (2) can be written in its real and imaginary parts:

$$u_{\mathbf{k}}(\mathbf{r}) = \alpha_{\mathbf{k}}(\mathbf{r}) + i\beta_{\mathbf{k}}(\mathbf{r}), \tag{9}$$

the usefulness of this decomposition will be apparent in the following. By inserting Eq. (9) in Eq. (2) and identifying real and imaginary parts one gets the coupled equations

$$-\frac{\hbar^2}{2m}(\nabla^2\alpha - 2\mathbf{k}\cdot\nabla\beta - k^2\alpha) + \frac{\hbar^2}{2m^2}(\nabla m)\cdot(\nabla\alpha - \mathbf{k}\beta) + (V-E)\alpha = 0, \tag{10}$$

$$-\frac{\hbar^2}{2m}(\nabla^2\beta + 2\mathbf{k}\cdot\nabla\alpha - k^2\beta) + \frac{\hbar^2}{2m^2}(\nabla m)\cdot(\nabla\beta + \mathbf{k}\alpha) + (V-E)\beta = 0, \tag{11}$$

The subscript $\mathbf{k}$ on α, β, and E has been dropped, and will be implicitly understood throughout the following. For any $\mathbf{k}$, the above are the eigenvalue-eigenvector equations of the $\mathbf{k}$ fiber of the Hamiltonian, which is characterized by a pure point spectrum, that is, by an infinity of eigenstates $E_n(\mathbf{k})$.[14] In this eigenvalue problem one can multiply both sides of the equality by m^2, but this also puts a position-dependent factor in front of E, the eigenvalue, thereby leading to a complicated problem. Perturbative techniques around the constant mass solution are possible, but must be developed with care (see Sec. IV). [In the perturbative approach, self-adjointness of the operators does not come out naturally if the correct Hilbert space is not identified (see the following section).] Our analytical approach, on the contrary, does not suffer any limitation. Each $E_n(\mathbf{k})$, for n fixed, corresponds to an energy band of the system; we now show how to compute the spectrum of such fibers in an exact way.

Thanks to their periodicity properties, the real functions α, β, m, and V can be written as trigonometric series in terms of their trigonometric moments $\alpha_{\mathbf{g}}$, $\beta_{\mathbf{g}}$, $m_{\mathbf{g}}$, and $V_{\mathbf{g}}$, where $\mathbf{g}$ are vectors in the reciprocal lattice $\mathcal{G}$: by letting h be any of these periodic functions, we write

$$h(\mathbf{r}) = \sum_{\mathbf{g}\in\mathcal{G}} h_{\mathbf{g}}\, e^{-i\mathbf{g}\cdot\mathbf{r}}. \tag{12}$$

The generic $\mathbf{g}$ moment $h_{\mathbf{g}}$ is defined by

$$h_{\mathbf{g}} = \frac{1}{W}\int e^{i\mathbf{g}\cdot\mathbf{r}}\, h(\mathbf{r})\, d\mathbf{r}, \tag{13}$$

W being the volume of the integration region, which is defined by the periodicity of the system. The reality requirement obviously corresponds to $h^*_{\mathbf{g}} = h_{-\mathbf{g}}$. We will assume that m and V are such that only a finite number of their trigonometric moments are non-null. One now employs the trigonometric expansions (12) into Eqs. (10) and (11). Multiplication by m^2 in these equations does not constitute a problem in this approach, and solves the problem of position-dependent denominators.

Alternatively, one could employ the different assumption that the trigonometric expansion of $m^{-1}(\mathbf{r})$ is finite. In this case, no denominators appear in Eqs. (10) and (11), and the resulting equations can be treated in the same way as we are now going to do under the former assumption.

The net effect of the manipulations leading to Eqs. (10) and (11) is to produce a lattice model completely analogous to the original Hamiltonian (1).[4] [The word *lattice* is here used to signify the Hilbert space $l^2(Z^N)$ of square-integrable functions defined only on discrete positions.] In order to understand the structure of the lattice Hamiltonian it is crucial to look at the action of the operators involved in (10) and (11). The operators ∇^2, $\mathbf{k}\cdot\nabla$, k^2, act multiplicatively on each "mode number" $e^{-i\mathbf{g}\cdot\mathbf{r}}$. Since $\mathbf{g}$ now identifies a site in a lattice, the previous operators give "diagonal" contributions. On the contrary, factors such as $m(\mathbf{r})$, ∇m, and $V(\mathbf{r})$, all provide "couplings" between different sites. We remark that, thanks to our assumptions (and after multiplication by m^2), a finite number of trigonometric modes appears in front of the diagonal operators. Hence the range of such couplings is finite.

This fact can be expressed by defining the set $\mathcal{S}\subset\mathcal{G}$ such that two modes $\mathbf{g}$ and $\mathbf{g}'$ are coupled from Eqs. (10) and (11) if and only if $\mathbf{g}-\mathbf{g}'\in\mathcal{S}$. In the above notations (which are illustrated in Fig. 1) Eq. (10) takes the general form

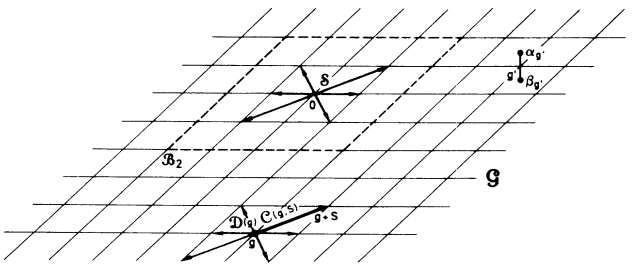

FIG. 1. Couplings in the lattice space $\mathcal{G}$. The components of the lattice eigenfunction at the site $\mathbf{g}'$ are $\alpha_{\mathbf{g}'}$ and $\beta_{\mathbf{g}'}$. The diagonal energy of the site $\mathbf{g}$ is indicated by $D(\mathbf{g})$. The site $\mathbf{g}$ is coupled to the state $\mathbf{g}+\mathbf{S}$ via the coupling $C(\mathbf{g},\mathbf{S})$, for any $\mathbf{S}\in\mathcal{S}$. $\mathcal{S}$ is the coupling set, centered at the origin $\mathbf{0}$. The box $\mathcal{B}_2$ is also shown.

$$D^{(\alpha)}(\mathbf{g},\mathbf{k})\alpha_{\mathbf{g}} + D^{(\beta)}(\mathbf{g},\mathbf{k})\beta_{\mathbf{g}} + \sum_{\mathbf{s}\in\mathcal{S}}[C^{(\alpha)}(\mathbf{g},\mathbf{s},\mathbf{k})\alpha_{\mathbf{g}+\mathbf{s}} + C^{(\beta)}(\mathbf{g},\mathbf{s},\mathbf{k})\beta_{\mathbf{g}+\mathbf{s}}] = E\alpha_{\mathbf{g}}, \tag{14}$$

for any lattice vector $\mathbf{g}$. The coefficients D (diagonal) and C (coupling) can be explicitly constructed as functions of the trigonometric moments of V and m. A similar equation follows from (11):

$$\tilde{D}^{(\alpha)}(\mathbf{g},\mathbf{k})\alpha_{\mathbf{g}} + \tilde{D}^{(\beta)}(\mathbf{g},\mathbf{k})\beta_{\mathbf{g}} + \sum_{\mathbf{s}\in\mathcal{S}}[\tilde{C}^{(\alpha)}(\mathbf{g},\mathbf{s},\mathbf{k})\alpha_{\mathbf{g}+\mathbf{s}} + \tilde{C}^{(\beta)}(\mathbf{g},\mathbf{s},\mathbf{k})\beta_{\mathbf{g}+\mathbf{s}}] = E\beta_{\mathbf{g}}, \tag{15}$$

with the corresponding coefficients $\tilde{D}$ and $\tilde{C}$.

Let us now consider "boxes" in the lattice Fourier space defined by writing the reciprocal vectors on a dual basis $\{\mathbf{e}_j\}$,

$$\mathbf{g} = n_1\mathbf{e}_1 + \cdots + n_N\mathbf{e}_N, \tag{16}$$

and identifying the box $\mathcal{B}_M$ as the vectors such that $|n_j| \le M\ \forall j$. We will also call $\mathcal{B}_M$ the set of moments $\alpha_{\mathbf{g}}$ and $\beta_{\mathbf{g}}$ for $\mathbf{g}\in\mathcal{B}_M$. First of all, not all such vectors are independent: the reality condition for α (β) immediately implies $\alpha_{-\mathbf{g}} = \alpha^*_{\mathbf{g}}$ ($\beta_{-\mathbf{g}} = \beta^*_{\mathbf{g}}$). Moreover, particular symmetry conditions may hold, which also restrict the set of independent vectors. All these conditions must be checked *a priori*. A particular case of this procedure will be shown in the next section; we continue here on the most general footing.

These boxes in reciprocal space are needed for a sort of "exact truncation" of the problem to a finite subspace. We will show how to derive consistency relations on such finite subspaces which constrain the physical variables (eigenvalues, eigenfunctions) within exact bounds, which get exponentially sharper as the box dimension increases. So far the theory has been standard manipulation, we will now enter the two main steps of our method: the first, "dynamical" (where we define the concept of missing moments); the second, analytical (where we find such missing moments).

Dynamics comes into play once symmetries have been properly taken into account. Equations (14) and (15) provide new linear constraints on the box moments, in terms of the coefficients $C, D, \tilde{C}, \tilde{D}$, and of the energy E. One is always able to find a smaller set of linearly independent moments, which can be enumerated: we will denote such moments with μ_i, $i = 0,\ldots,I$. Their number, $I+1$, in general depends on M, and on the structure of the coupling set $\mathcal{S}$. One can equivalently say that the μ_i are the least set of α and β moments required to linearly produce all the moments of the box $\mathcal{B}_M$:

$$\begin{aligned} \alpha_{\mathbf{g}} &= \sum_{i=0}^{I} A_i(\mathbf{g},E)\mu_i, \\ \beta_{\mathbf{g}} &= \sum_{i=0}^{I} B_i(\mathbf{g},E)\mu_i, \quad \forall \mathbf{g}\in\mathcal{B}_M. \end{aligned} \tag{17}$$

The coefficients A_i and B_i can be explicitly calculated as functions of E from Eqs. (14) and (15). The number of unknowns has now been reduced to $I+2$, the *missing moments* μ_i, and the energy E: dynamics has been taken into account. [By imposing proper normalization conditions, one of the missing moments can be eliminated as a linear function of the others. Yet, this numerically relevant procedure does not change the structure of Eqs. (17).]

The final and decisive step is provided by analysis: owing to the representation (13), the moments $\alpha_{\mathbf{g}}$ and $\beta_{\mathbf{g}}$ *cannot* be any set of complex numbers; on the contrary, they must satisfy rather stringent requirements, corresponding in the one-dimensional case to the traditional Hankel-Hadamard inequalities.[15] As the case of α and β moments is perfectly symmetric, we will only derive the set of inequalities for α. The real periodic function $\alpha(\mathbf{r})$, is characterized by a minimum value over the region of periodicity. Then we can take an arbitrarily large constant Q such that $f(\mathbf{r}) = \alpha(\mathbf{r}) + Q$ is a positive function. It is then also true that

$$f(\mathbf{r})\left|\sum_{\mathbf{g}\in\mathcal{B}} c_{\mathbf{g}}e^{i\mathbf{g}\cdot\mathbf{r}}\right|^2 \ge 0, \tag{18}$$

for any choice of the set of complex numbers $c_{\mathbf{g}}$, and for any box $\mathcal{B}$. By integrating the inequality (18) one obtains a relation involving the trigonometric moments of f:

$$\sum_{\mathbf{g}\in\mathcal{B}}\sum_{\mathbf{g}'\in\mathcal{B}} c^*_{\mathbf{g}}c_{\mathbf{g}'}f_{\mathbf{g}'-\mathbf{g}} \ge 0. \tag{19}$$

By introducing the matrices $T_{\mathbf{g},\mathbf{g}'} = f_{\mathbf{g}'-\mathbf{g}}$ (for different boxes $\mathcal{B}$) the above inequalities are equivalent to the positivity of these matrices, and can hence be rewritten in terms of determinants. For our purposes, though, the linear form (19) is more convenient.

Since the moments of f are exactly the same as the moments of α, except for $\mathbf{g} = \mathbf{0}$, for which $f_{\mathbf{0}} = \alpha_{\mathbf{0}} + Q$, one finally obtains the desired set of inequalities for the moments of the solution of the Schrödinger equation:

$$\sum_{\mathbf{g}\in\mathcal{B}}\sum_{\mathbf{g}'\ne\mathbf{g}\in\mathcal{B}} c^*_{\mathbf{g}}c_{\mathbf{g}'}\alpha_{\mathbf{g}'-\mathbf{g}} \ge -(Q+\alpha_{\mathbf{0}})\sum_{\mathbf{g}\in\mathcal{B}}|c_{\mathbf{g}}|^2. \tag{20}$$

The inequalities (20) must always be true, as they are a sort of consistency condition dictated by analysis. When dynamics is input via Eq. (17), expressing the box moments $\alpha_{\mathbf{g}}$ in terms of the missing moments μ_i, a new set of inequalities is produced, which are linear in the missing moments μ_i, and nonlinear in the energy E:

$$\sum_{i=0}^{I} \mu_i \left(\sum_{\mathbf{g}\in\mathcal{B}} \sum_{\mathbf{g}'\neq\mathbf{g}\in\mathcal{B}} c_{\mathbf{g}}^* c_{\mathbf{g}'} A_i(\mathbf{g}'-\mathbf{g}, E) + [Q + A_i(\mathbf{0}, E)] \sum_{\mathbf{g}\in\mathcal{B}} |c_{\mathbf{g}}|^2 \right) \geq 0. \quad (21)$$

These final sets of inequalities are the cornerstone for the solution of the spectral problem: at any fixed (arbitrary) value of E we carefully choose a set of vectors $c_{\mathbf{g}}$ in order that one of the exclusive opportunities holds: (i) the set of inequalities (21) has no solution, and hence the chosen value E is *unfeasible*, or (ii) a set of missing moments μ_i which satisfies all the inequalities (21) is found. This latter set of moments, as well as the value of E, is then defined *feasible*. The optimal procedure to choose $c_{\mathbf{g}}$ values is explained in Refs. 16 and 4.

Doing as prescribed above, one determines the extrema of the region of values of E for which a solution of the inequalities (21) exists, for any vector $c_{\mathbf{g}}$. (The set of feasible values of E turns out to be an interval if the box $\mathcal{B}$ is not too small.) This region depends on the box $\mathcal{B}$, and provides *exact* upper and lower bounds to the unknown eigenvalue. The linear programming techniques implicit in (21) also bring about exact bounds to the missing moments. As the size of $\mathcal{B}$ increases, these bounds exponentially shrink around the true eigenvalue E, and the related missing moments. The full solution of the problem is then obtained by computing the remaining box moments via Eqs. (17). The example of the next section will further clarify this technique.

III. MODULATED SEMICONDUCTOR SUPERLATTICES

Let us now get back to the specific example of modulated semiconductor superlattices described in the Introduction. The theory of electronic states in these structures is conveniently carried out in the so-called *envelope-function approximation*.[5,6,17] The essential feature of this approximation is to leave unperturbed the atomic scale physical characteristics (host semiconductor band edge and effective mass), and to describe the large period superstructure via a slowly varying envelope function $F(\mathbf{r})$. For instance, in a multiwell structure, the electron wave function is written

$$\psi^S(\mathbf{r}) = \sum_j F_j^S(\mathbf{r}) u_j^S(\mathbf{r}), \quad (22)$$

where u_j^S are the periodic parts of the Bloch wave functions at $k = 0$ (Γ point) for the bulk S material, where S is either one of the semiconductor components, and the sum over j involves different bands. In the simplest case, one can assume that the interaction governing $F(\mathbf{r})$ is localized at the sharp interfaces between different S materials: as a consequence, dynamics can be rendered by appropriate matching conditions for F.[2,5]

Modulated semiconductor superlattices are a notable case for which the last approximation fails, as they do not present sharp interfaces. The envelope-function description can nevertheless be maintained, by writing

$$\psi(\mathbf{R}) = \sum_j F_j(\mathbf{R})\, u_j^{\mathbf{R}}(\mathbf{r}), \quad (23)$$

where $\mathbf{r} = \mathbf{R} - \boldsymbol{l}$ is the difference between $\mathbf{R}$ and the closest lattice vector $\boldsymbol{l}$. While $\mathbf{r}$ is a vector on the atomic scale, $\mathbf{R}$ ranges on the much larger superperiod scale. Since the components of the superlattice now vary continuously with $\mathbf{R}$, by $u_j^{\mathbf{R}}(\mathbf{r})$ we now mean the $k = 0$ periodic part of the (bulk) Bloch wave function for the jth band of the material which is found around the position $\mathbf{R}$. The electronic states F_j are then governed by an effective Hamiltonian H: $(HF)_j = \lambda F_j$. H is usually a matrix differential operator, as it couples different Bloch functions u_j. This is typically the case of valence-band levels, where coupling between light- and heavy-hole states is required. The structure of modulated semiconductor superlattices and the relevant notations are illustrated in Fig. 2.

Let us now focus on the electron conduction band in III-V semiconductor superlattices: as this band is well separated from the others one can safely use a scalar envelope function $F(R)$. The theory of valence-band levels is also possible by our method, although more complicated. Since the envelope function depends only on the growth direction of the superlattice, R can be taken as a scalar variable. Let P be the length of the superperiod of the specimen. The effective Hamiltonian H for F assumes the form of a periodic Schrödinger operator, discussed in Sec. II:

$$H = -\frac{\hbar^2}{2}\left(\nabla \frac{1}{m} \nabla\right) + Q_c E_g(R) + U, \quad (24)$$

where Q_c is the conduction-band offset value, $E_g(R)$ the energy gap for the material at R, and U allows for the possibility of an external field. In the next section we show that to a good approximation one can write

$$Q_c E_g(R) = \delta \cos(gR) \quad (25)$$

and

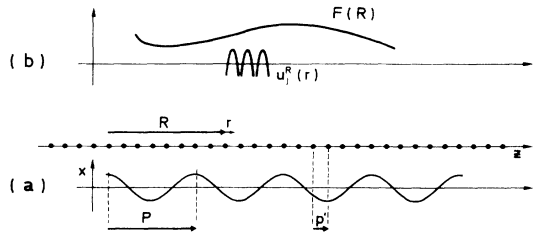

FIG. 2. Geometry and notations for modulated semiconductor superlattices. In (a) the aluminum ratio x is plotted vs the growth direction z of the superlattice. The vector $\mathbf{P}$ indicates the periodicity of the modulation, and the vector $\mathbf{p}'$ the local periodicity of the crystalline lattice. In (b), the envelope function $F(R)$ is shown, together with the (schematic) local Bloch functions $u_j^R(r)$ of $Al_xGa_{1-x}As$.

$$m(R) = m_0 + \Delta\cos(gR), \tag{26}$$

where $g = 2\pi/P$, and δ, m_0, and Δ are structural constants.

Let us now employ the techniques of Sec. II to solve the spectral problem (24)–(26), with $U = 0$, using the notation $\theta = gR$ to emphasize its periodic nature. The decomposition (9), as well as Eqs. (10) and (11) immediately apply to this case. On the other hand, thanks to (25) and (26), the problem is characterized by an additional symmetry: it is easy to show that the eigenfunctions $u(\theta)$ satisfy

$$\alpha(\theta) = \alpha(-\theta), \quad \beta(\theta) = -\beta(-\theta), \tag{27}$$

since this form is required for H to be a symmetric operator. It is also immediate to verify that this form is preserved by the action of H, and hence defines a correct Hilbert space for the system. The moment representations (12) enjoy the corresponding symmetries $\alpha_n = \alpha_{-n} = \alpha_n^*$ and $\beta_n = ib_n$, with $b_n = -b_{-n} = b_n^*$. Using these representations in Eqs. (10) and (11) one gets two coupled lattice Hamiltonian equations of the form (14) and (15):

$$(\Gamma^1 + \Gamma^2 n^2)\alpha_n + [\Gamma^3 + (n-1)\Gamma^4 - (n-1)^2\Gamma^4]\alpha_{n-1} + [\Gamma^3 - (n+1)\Gamma^4 - (n+1)^2\Gamma^4]\alpha_{n+1}$$

$$+\Gamma^5(\alpha_{n-2} + \alpha_{n+2}) + \Gamma^6(\alpha_{n-3} + \alpha_{n+3}) + n\Gamma^7 b_n + [(n-1)\Gamma^8 - \Gamma^9]b_{n-1} + [(n+1)\Gamma^8 + \Gamma^9]b_{n+1} = 0, \tag{28}$$

$$(\Gamma^1 + \Gamma^2 n^2)b_n + [\Gamma^3 + (n-1)\Gamma^4 - (n-1)^2\Gamma^4]b_{n-1} + [\Gamma^3 - (n+1)\Gamma^4 - (n+1)^2\Gamma^4]b_{n+1}$$

$$+\Gamma^5(b_{n-2} + b_{n+2}) + \Gamma^6(b_{n-3} + b_{n+3}) + n\Gamma^7\alpha_n + [(n-1)\Gamma^8 - \Gamma^9]\alpha_{n-1} + [(n+1)\Gamma^8 + \Gamma^9]\alpha_{n+1} = 0. \tag{29}$$

The constants Γ^j, $j = 1, \ldots, 9$ are explicit functions of E, k, and the structural constants, as shown in Table I.

Thanks to the symmetries of α_n, b_n, a careful analysis of Eqs. (28) and (29) shows that the infinite set of α and β moments can be generated recursively as a function of $\alpha_0, \alpha_1, \alpha_2, b_1, b_2, b_3$, which constitute the *missing moments set*. This leads to the general equation (17), with $\mathrm{g} = n$, $I = 5$, and where the coefficients A_i are also obtained recursively from Eqs. (28) and (29). It is noteworthy that, in one-dimensional cases like the present, a finite set of missing moments is capable of generating the infinite, full sets of moments, and not only a finite box $\mathcal{B}$.

To obtain the necessary set of Hankel-Hadamard inequalities (20) one considers nevertheless a finite box $\mathcal{B}_M$ in moment space, which is now defined by $0 \le n \le M$. When the proper algebraic steps leading to Eq. (21) have been taken, one is left with an infinite set of inequalities for the missing moments, and the energy E, parametrized by the complex vectors $\mathbf{c}_n$. A straightforward application of the numerical techniques described in the previous section then leads to the determination of the feasible regions of E, which are nested for increasing M. The numerical results are shown in the next section for two particular choices of physical parameters.

TABLE I. Constants Γ^j appearing in the lattice equations (28) and (29).

$\Gamma^1 = \hbar^2k^2m_0 + 2m_0\Delta\delta - E(2m_0^2 + \Delta^2)$
$\Gamma^2 = \hbar^2g^2m_0$
$\Gamma^3 = \frac{1}{2}\hbar^2k^2\Delta + m_0^2\delta + \frac{3}{4}\Delta^2\delta - 2Em_0\Delta$
$\Gamma^4 = -\frac{1}{2}\hbar^2g^2\Delta$
$\Gamma^5 = m_0\Delta\delta - \frac{1}{2}E\Delta^2$
$\Gamma^6 = \frac{1}{4}\Delta^2\delta$
$\Gamma^7 = -2\hbar^2km_0g$
$\Gamma^8 = \hbar^2k\Delta^2g^2$
$\Gamma^9 = -\hbar^2k\Delta g$

IV. ELECTRONIC STATES: NUMERICAL RESULTS

Let us now specialize the previous theory to two real examples. Via the MBE technique, successive layers of $Al_xGa_{1-x}As$ have been deposed in the growth direction [001] (z axis) of a superlattice. The MBE technique has been so improved that it is now possible to modulate the aluminum ratio x from layer to layer as a function of z. In a particular superlattice (which we will denote SL No. 1),[12] x was varied sinusoidally between 0.2 and 0.5, with a period of 500 Å. 80 such periods were deposed.

The bulk $k = 0$ energy gaps at the temperature of 0 K (Ref. 18) are given by a quadratic approximation in x, which takes the values $E_g = 1.747$ eV for $x = 0.2$, and $E_g = 2.157$ eV for $x = 0.5$. It must be noticed, however, that the conduction-band minimum for $x > 0.45$ is no longer at the Γ point. We will nevertheless use the gap at the center of the Brillouin zone. In the x range between 0.2 and 0.5 one can assume a linear variation of E_g, of the form $E_g(x) = E(0.2) + [(x-0.2)/0.3[E(0.5) - E(0.2)]$. Since x varies sinusoidally with z, we can now write $E_g(z) = E_c + \delta\cos(gz)$. In the following, we will take the zero of the energy axis at E_c, that is, at the center of the oscillation of E_g. The potential energy acting on electrons (holes) in conduction (valence) bands is given by the product of E_g times the offset factor Q_c ($Q_v = 1 - Q_c$). We can assume that this value is constant through the oscillation. As a first approximation, one can take the value valid in the case of sharp interfaces between $Al_{0.2}Ga_{0.8}As$ and $Al_{0.5}Ga_{0.5}As$ materials,

TABLE II. Structural constants for two superlattices.

	SL 1	SL 2
δ	2.204×10^{-13} erg	1.120×10^{-13} erg
m_0	2.133×10^{-28} g	2.130×10^{-28} g
Δ	1.530×10^{-29} g	7.652×10^{-30} g
g	1.256×10^{6} cm^{-1}	6.283×10^{6} cm^{-1}

$Q_c = 0.67$.[10] Our following considerations will enable us to determine this factor from matching of experimental data. The effective Hamiltonian potential energy takes then the form (25), where $\delta = Q_c[E(0.5) - E(0.2)]/2$. The numerical value of δ is reported in Table II.

Similarly, a linear variation can been assumed for the mass m as a function of the aluminum ratio x, so that the modulation of the mass in the z direction is also sinusoidal, and it ranges around the value of $m_0 = 2.133 \times 10^{-28}$ g with an amplitude $\Delta = 1.53 \times 10^{-29}$ g. In this way, one obtains Eq. (26), and the full effective Hamiltonian for the envelope function is produced.

We have applied the method explained in Secs. II and III to find the spectrum of this Hamiltonian. The results of the computation of electronic levels are shown in Table III. These values are obtained for $k = 0$, but the variation within the first Brillouin zone of the superlattice is less than the number of digits reported: the minibands here are very tight.

Internal miniband structure begins to appear when the superperiod gets smaller and smaller. In order for this to be technically feasible, a smaller variation of the alloy ratio x is to be considered. We can hence consider a second set of physical parameters, corresponding to a modulation of x between $x = 0.3$ and $x = 0.45$, taking place with a superperiod of 100 Å. The related parameters are reported in Table II, and are labeled as superlattice (SL) No. 2. The dispersion relations $E(k)$ here are more significant, since the shorter period and the lower barrier allow a more significant tunneling to take place. We are considering a one-dimensional problem, and hence we expect the electronic levels to be monotonic functions of k, the superlattice quasimomentum. This latter is defined in relation to the superperiod of the material, and for this reason, it is of the order of 10^6 cm^{-1}. It also corresponds to the "global" **k** vector in the [001] direction, in the envelope-function approximation. In Fig. 3, we see that the energy bands described by $E(k)$, $k = 0, \pi/P$ are very

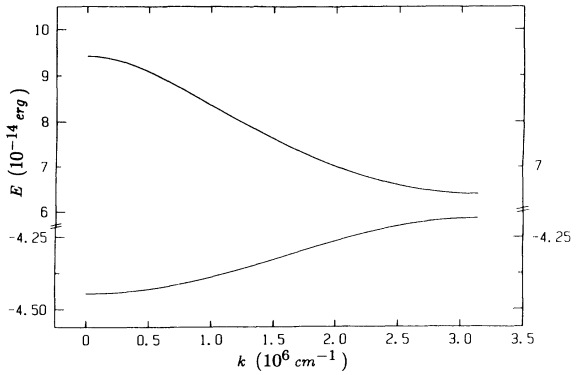

FIG. 3. Band structure of superlattice No. 2. The two lowest minibands are plotted.

narrow, of the order of meV. This is explained by the fact that such typical "minibands" originate from tunneling of wave functions through the potential barriers created by the oscillating effective potential.

It is to be remarked that our diagonalization procedure offers *exact* values for the energy bands: to show this fact, in Table IV we exhibit the $k = 0$ exact upper and lower bounds to the eigenenergy of the lowest band, as a function of the box size M (see Sec. III). Since increasing this number gives more stringent inequalities, the bounds get better and better at an exponential rate.

Via the same technique it is possible to compute the band structure as a function of all the constants appearing in the theory; in particular, we considered the most relevant role of the potential amplitude δ. Since the global oscillation of E_g is rather well known, δ is basically determined by the offset Q_c, whose value is imprecisely known. The values reported in the literature vary between $Q_c = 0.5$ (Ref. 11) and $Q_c = 0.85$;[8] we therefore calculated the three lowest energy bands in a range of values of δ which contains such extreme values. The resulting bands are plotted in Fig. 4, showing their obvious narrowing for increasing δ. The variation of the band energies with δ is significant, and should allow us to determine the value of Q_c from experimental absorption spectra (revealing the transition energies), via an analysis similar to that of Ref. 10. This analysis must be completed by computing hole valence states, which can also be done via our procedure (in a matricial Hamiltonian form when necessary).

TABLE III. Electronic levels of SL No. 1 for $k = 0$. The conversion constant is 1 eV=1.6022×10^{-12} erg.

l	E_l (eV)
0	−0.1240
1	−0.0973
2	−0.0713
3	−0.0463
4	−0.0221

TABLE IV. Lower ($E_<$) and upper ($E_>$) bounds to the electronic lowest-energy state of SL No. 2, as a function of the box size M, for $k = 0$.

M	$E_<$ (10^{-14} erg)	$E_>$ (10^{-14} erg)
6	−4.48	−4.40
7	−4.444	−4.432
8	−4.4379	−4.4371
9	−4.437515	−4.437490

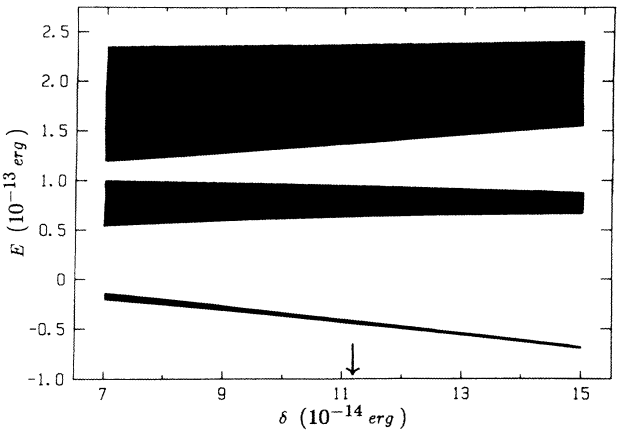

FIG. 4. Band structure of superlattice No. 2 as a function of δ. This corresponds to a variation in the value of Q_c. The value of δ corresponding to $Q_c = 0.67$ is indicated by an arrow. The three lowest minibands are plotted.

Finally, the band structure can also be computed as a function of Δ, the oscillation in the effective mass [Eq. (26)], in a quite analogous way. In fact, let us first neglect this effect by posing $\Delta = 0$—that is, by considering a constant average effective mass. We can compute the band structure, also via our technique, and denote by $E(k,0)$ the lowest energy band, say, for the superlattice No. 2. We then compute the true energy band, with $\Delta \neq 0$: $E(k,\Delta)$, and study the difference $E(k,\Delta) - E(k,0)$ as a function of k, and Δ. This difference is plotted in Fig. 5. The arrow indicates the value

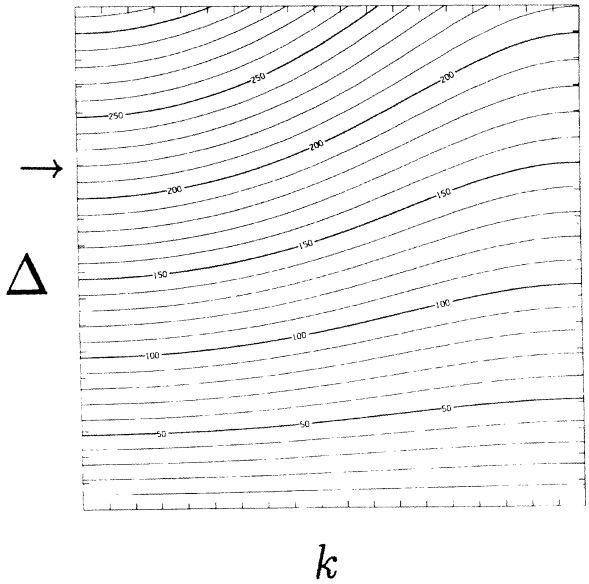

FIG. 5. Difference $E(k,\Delta) - E(k,0)$ for the lowest-energy band of superlattice No. 2 as a function of k and Δ. The horizontal k axis ranges between 0 and $\frac{\pi}{T} = 3.141 \times 10^6$ cm^{-1}. The vertical Δ axis ranges between 0 and 11.5×10^{-30} g, the arrow indicates the value $\Delta = 7.652 \times 10^{-30}$ g typical of SL No. 2 (Table II). Level curves are in units of 10^{-18} erg.

of Δ typical of SL No. 2 (Table II). Even if one has that Δ/m_0 is of the order of a few percent, it induces a shift of the energy bands which is nonlinear in k. This shows the importance of taking into account the effect of variable mass via an exact procedure. To appreciate this fact even more, we now resort to a more traditional approach, to compare its prediction with our results.

A possible approach to the spectral problem (24)–(26) is the following. The position-dependent denominator $\frac{1}{m}$ can be approximately written as $m_0^{-1}(1 - \Delta m_0^{-1} \cos gR)$ plus terms of second order in Δ. This leads us to consider an approximate k-fiber Hamiltonian of the form

$$H_k = -\frac{\hbar^2}{2m_0}\left(1 - \frac{\Delta}{m_0}\cos(gR)\right)(-k^2 + 2ik\nabla + \nabla^2) - \frac{\hbar^2}{2m_0}\frac{\Delta}{m_0} g \sin(gR)(ik + \nabla) + \delta\cos(gR). \quad (30)$$

The above Hamiltonian is also self-adjoint on the domain of $u(gR)$ defined in (27),[19] and hence defines a good approximation to the exact problem. A basis for the Hilbert space (27) is easily written as $\psi_0 = 1$, $\psi_{2n} = \frac{1}{\sqrt{2}}(e^{ingR} + e^{-ingR})$, and $\psi_{2n-1} = \frac{1}{\sqrt{2}}(e^{ingR} - e^{-ingR})$. We can then take a truncated basis set $n = 0, \ldots, N$ and restrict H_k to such subspace. The matrix elements are readily computed and the resulting finite order matrix can be diagonalized numerically.

This provides us with an interesting comparison with our previous results. We noticed that—for the physical parameters corresponding to the superlattices above—the lower-energy bands results were practically stable for matrix dimensions of order 10. This is due to the small value of the perturbative constant $\frac{\Delta}{m_0}$ in Eq. (30). Also due to this fact, results were quite consistent with the exact bounds reported before; yet the superiority of the moment approach can be noticed.

First of all, due to the nonlinear effect in k noticed above, the approximate matrix formulation should work at its best for $k = 0$. We hence considered the lowest-energy band, in the case of superlattice No. 2, and we computed the the eigenenergy, as a function of the matrix dimension—Table V, which is to be compared to Table IV. In the first column of Table V we report the result that one would have obtained by setting $\Delta = 0$ (thereby neglecting altogether the variation in the effective mass). The second column reports the diagonaliza-

TABLE V. Lowest-energy band of SL No. 2, at $k = 0$, with $\Delta = 0$ (first column), $\Delta = 7.652 \times 10^{-30}$ g (second column), obtained by diagonalization of matrices of order N. These results are to be compared with the exact results of Table IV.

N	E (10^{-14} erg)	E (10^{-14} erg)
1	−4.29	−4.29
2	−4.45	−4.44
8	−4.459 9	−4.438 4
9	−4.459 922	−4.438 417
20	−4.459 922	−4.438 417

tion values with $\Delta = 7.652 \times 10^{-30}$ g.

We notice that these values converge rather quickly to their asymptotic value, but that such an asymptotic value is in both cases *unfeasible*; that is, surely, incorrect. For example, the value obtained with $N = 8$ is out of the feasibility region delimited by using the same number of moments, and the exact method. It is to be remarked that, while in this case the agreement is good, we expect it to get worse as the ratio Δ/m_0 increases. Higher-order perturbative approximations could correct this tendency only initially.

In general, we believe that the exact method will be a viable tool in the very general class of operators here considered, superlattices being only an illustrative one-dimensional example. Moreover, as we have stated already, obtaining exact bounds on the energy bands can also be a critical test of other solution procedures.

V. CONCLUSIONS

We have presented an exact diagonalization scheme which can be applied to any periodic Schrödinger operator with a finite number of harmonics, in spaces of arbitrary dimension, and also for the case of variable mass. This case is particularly significant in solid-state physics, where the effective mass is given by the local band curvature, and can therefore depend on position. The same theory applies to quantum systems defined on a lattice, where the coupling between different sites has a finite range.

Our theory is based on the classical theory of moments, and allows us to derive exact upper and lower bounds on the energy bands of these systems. As these bounds can be made arbitrarily tight, the spectral problem can be considered exactly solved.

To illustrate the present techniques in a physically significant example, we have computed the electronic states of modulated $Al_xGa_{1-x}As$ semiconductor superlattices. The exact results obtained by our technique permit us to master the important physical effects taking place in these materials. In this context, by the techniques of Secs. II and III suitably generalized to a matrix Hamiltonian formalism, one is also able to treat hole energy spectra, in valence bands. More harmonics can be also kept in the effective-mass expansion, and their effect on the energy bands studied in detail.

We envision that this work will provide the solution of many physical problems, in the solid-state domain (e.g., to be used like a tool in band-gap engineering) and more generally in the quantum mechanics of periodic systems.

ACKNOWLEDGMENTS

Service de Physique Théorique is a Laboratoire de la Direction des Sciences de la Matière du Commissariat à l'Énergie Atomique.

[1] W.A. Harrison, Phys. Rev. **123**, 81 (1961).
[2] D.J. Ben Daniel and C.B. Duke, Phys. Rev. **152**, 683 (1968).
[3] M. Reed and B. Simon, *Methods of Modern Mathematical Physics, Vol. IV. Theory of Operators* (Academic, New York, 1978), see Theorem XIII.87, p. 288.
[4] C.R. Handy, G. Mantica, and J. Gibbons, Phys. Rev. A **39**, 3256 (1989).
[5] G. Bastard, Phys. Rev. B **24**, 5693 (1981); **25**, 7584 (1982).
[6] M. Altarelli, Phys. Rev. B **28**, 8842 (1983).
[7] See, for instance, *Heterojunction Band Discontinuities: Physics and Device Applications*, edited by F. Capasso and G. Margaritondo (Elsevier, Amsterdam, 1987).
[8] R. Dingle, W. Wiegmann, and C.H. Henry, Phys. Rev. Lett. **33**, 837 (1974); R. Dingle, Festkörperprobleme **15**, 21 (1975).
[9] H. Shelton and A.Y. Cho, J. Appl. Phys. **37**, 3544 (1986).
[10] G. Duggan, in *Heterojunction Band Discontinuities: Physics and Device Applications* (Ref. 7).
[11] R.C. Miller, A.C. Gossard, D.A. Kleinman, and O. Munteanu, Phys. Rev. B **29**, 3740 (1984).
[12] S. Mantica, thesis, University of Pavia, 1989.
[13] C.R. Handy, L. Luo, G. Mantica, and A.S. Msezane, Phys. Rev. A **38**, 490 (1988).
[14] M. Reed and B. Simon, *Methods of Modern Mathematical Physics, Vol. IV* (Ref. 3), see Sec. 16, pp. 279ff.
[15] J.A. Shohat and J.D. Tamarkin, *The Problem of Moments* (American Mathematical Society, Providence, RI, 1963).
[16] C.R. Handy, D. Bessis, and T.D. Morley, Phys. Rev. A **37**, 4557 (1988).
[17] J.N. Schulman, and G.W. 't Hooft, Phys. Rev. B **31**, 8041 (1985).
[18] A. Onton, Festkörperprobleme **13**, 59 (1973).
[19] M. Reed and B. Simon, *Methods of Modern Mathematical Physics, Vol. II. Fourier Analysis and Self-Adjointness* (Academic, New York, 1978), see Chap. X, pp. 135ff.